RESEARCH PAPER

Cell Adhesion & Migration 8:5, 499–508; September/October 2014; Published with license by Taylor & Francis Group, LLC

EDI3 links choline metabolism to integrin expression, cell adhesion and spreading

Michaela S Lesjak[1,†], Rosemarie Marchan[1,†,*], Joanna D Stewart[2], Eugen Rempel[3], Jörg Rahnenführer[3], and Jan G Hengstler[1]

[1]Department of Systems Toxicology; Leibniz Research Centre for Working Environment and Human Factors; Dortmund, Germany; [2]Centre for Biological Sciences; University of Southampton; Southampton, UK; [3]Department of Statistics; TU Dortmund University; Dortmund, Germany

[†]Both authors contributed equally to this work.

Keywords: EDI3, GDE5, glycerophosphodiesterase, choline metabolism, integrins, adhesion, spreading, migration, metastasis

Abbreviations: DAG, diacylglycerol; DHAP, dihydroxyacetone phosphate; ECM, extracellular matrix; EDI3, Endometrial carcinoma differential 3; ER, estrogen receptor; FN, fibronectin; GDE, glycerophosphodiesterase; GO, gene ontology; GPC, glycerophosphocholine; PA, phosphatidic acid; PC, phosphocholine; PKC, protein kinase C; PLD, phospholipase D; PtdCho, phosphatidylcholine.

Endometrial carcinoma differential 3 (EDI3) was the first member of the glycerophosphodiesterase (GDE) protein family shown to be associated with cancer. Our initial work demonstrated that endometrial and ovarian cancer patients with primary tumors overexpressing EDI3 had a higher risk of developing metastasis and decreased survival. Further analysis indicated that EDI3 cleaves glycerophosphocholine to choline and glycerol-3-phosphate, increases the levels of active PKC, and enhances the migratory activity of tumor cells. Despite these initial findings, EDI3 remained mainly uncharacterized. Therefore, to obtain an overview of processes in which EDI3 may be involved, gene array analysis was performed using MCF-7 breast cancer cells after EDI3 knockdown compared with a non-targeting control siRNA. Several biological motifs were altered, including an enrichment of genes involved in integrin-mediated signaling. More specifically, silencing of EDI3 in MCF-7 and OVCAR-3 cells was associated with reduced expression of the key receptor subunit integrin β1, leading to decreased cell attachment and spreading accompanied by delayed formation of cell protrusions. To confirm these results, we stably overexpressed EDI3 in MCF-7 cells which led to elevated integrin β1 expression associated with enhanced cell attachment and spreading - two processes critical for metastasis. In conclusion, our data provide further insight into the role of EDI3 during cancer progression.

Introduction

Recently, EDI3 (GDE5; GPCPD1) was identified as a key enzyme in choline metabolism.[1,2] Our initial studies showed that EDI3 cleaves the phosphodiester, glycerophosphocholine (GPC) to produce choline and glycerol-3-phosphate. We also showed that EDI3 regulates cellular migration via the PKCα signaling pathway. Choline metabolism has been intensively discussed in relation to several diseases, including neurological disorders,[3] liver disease,[4,5] and tumor progression.[6-10] With respect to the latter, recent studies have suggested that elevated choline metabolism, including increased phosphocholine (PC) levels, is associated with worse prognosis.[9,11-13] However, the mechanism of how higher PC levels contribute to cancer progression is not fully understood.

Many studies currently focus on choline kinase, the enzyme that phosphorylates choline to PC, as a potential target for therapy. Indeed, choline kinase has been reported to be elevated in several cancers, such as ovarian, breast, lung, colon and prostate.[10,14-17] However, our work suggests that EDI3, which via its enzymatic reaction is a potential source of choline for choline kinase, is also an important contributor to tumor progression. EDI3 expression was higher in the primary tumors of ovarian and endometrial cancer patients who went on to develop metastasis and had worse survival.[1] EDI3′s second product, glycerol-3-phosphate, is further metabolized to lysophosphatidic acid, phosphatidic acid and diacylglycerol. All three lipid products may act as membrane anchoring points, which can activate downstream signaling pathways, for example members of the Rho family of GTPases.[2] In addition, glycerol-3-phosphate, a key component of glycerophospholipids, is dehydrogenated to dihydroxyacetone phosphate (DHAP) by glycerol-3-phosphate dehydrogenase. DHAP in turn is isomerized to glyceraldehyde-3-phosphate, an important intermediate in several metabolic pathways, including glycolysis, which is upregulated in many cancers.

*Correspondence to: Rosemarie Marchan; Email: Marchan@ifado.de
Submitted: 03/19/2014; Revised: 05/12/2014; Accepted: 05/20/2014
http://dx.doi.org/10.4161/cam.29284

In our previous work, we focused on the enzymatic mechanism and discovered the migration phenotype out of a limited number of functional assays.[1] To obtain a comprehensive and unbiased overview of possible further EDI3 functions, in the present study we performed a gene array analysis of breast cancer cells after EDI3 knockdown. Among the several altered biological motifs, EDI3′s influence on integrin expression was one of the most interesting and relevant, especially considering EDI3′s role in migration – an integrin-mediated event. Integrins are heterodimeric α/β transmembrane receptors that connect the extracellular matrix (ECM) to intracellular signaling pathways and the actin cytoskeleton. Adhesion of cells to the ECM causes dynamic remodeling of the cytoskeleton thus influencing key processes, including cell migration, adhesion and spreading.

EDI3′s influence on key integrin receptor expression, and its importance to the migration process, prompted us to further investigate the role of EDI3 in cell adhesion. Using a combined knockdown and overexpression approach, we observed that EDI3 influences cellular processes closely associated with migration, namely cell attachment and spreading on a fibronectin matrix.

Results

Screening for EDI3 associated gene expression alterations

To study whether EDI3 had any influence on global gene expression, Affymetrix gene array and Qiagen Cancer Pathway Finder PCR array were performed to screen gene expression alterations after silencing EDI3 in MCF-7 cells as previously described.[1] Three independent experiments, each with three technical replicates, were performed using EDI3 siRNA #1 and a non-targeting control siRNA, resulting in 18 samples for

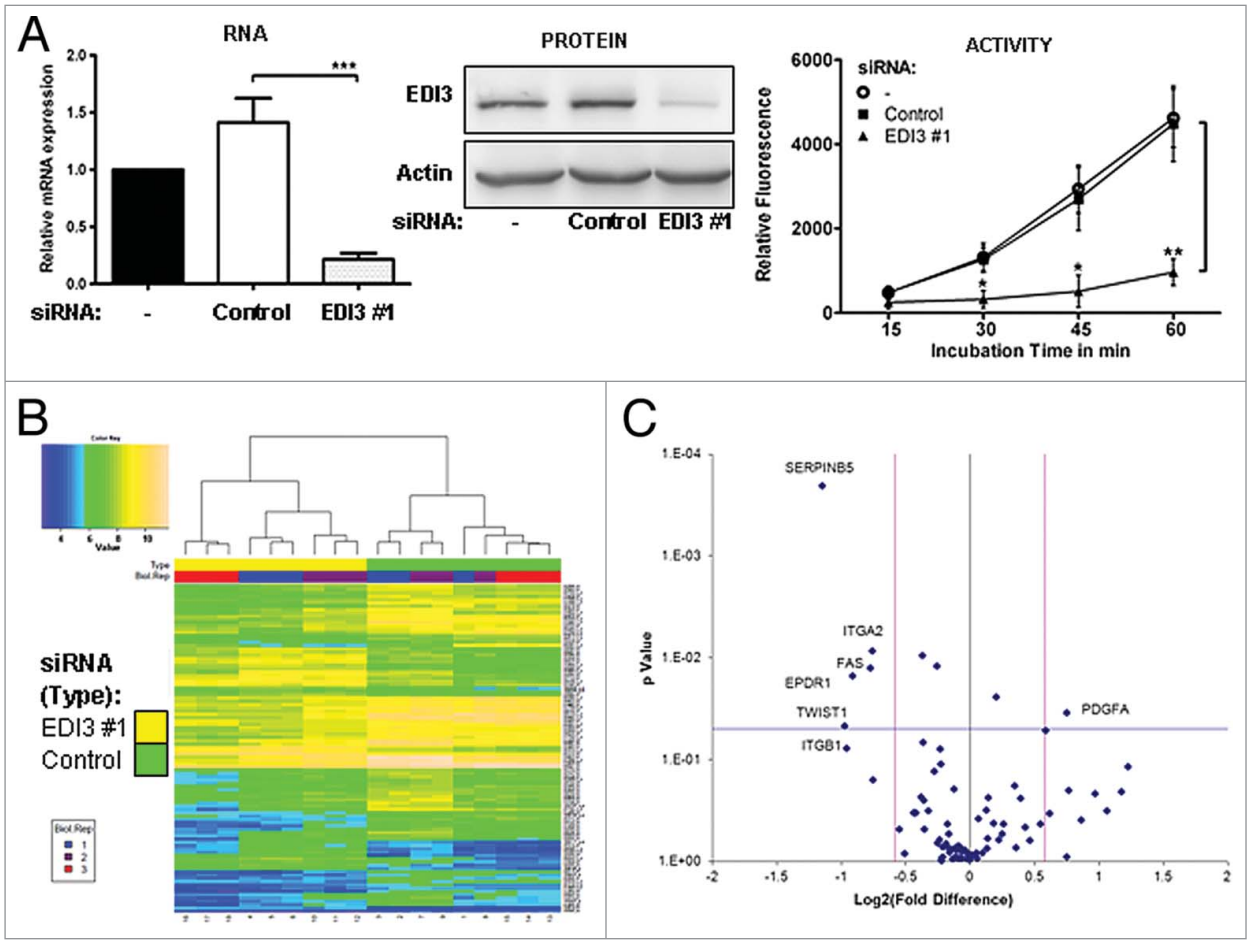

Figure 1. siRNA knockdown of EDI3 induces gene expression alterations important for adhesion and migration. (**A**) Quantitative real-time PCR, western blot analyses and spectrophotometric EDI3 activity assays using total cell lysates obtained from MCF-7 cells treated with control or specific EDI3 siRNA revealed a knockdown efficiency of approximately 80%. (**B**) Heatmap analysis comparing EDI3 siRNA knockdown (left side of map, numbered below as 4–6, 10–12, 16–18) in MCF-7 cells to controls transfected with non-targeting siRNA (right side of map, numbered below as 1–3, 7–9, 13–15). The color within the heat map represents the raw normalized gene expression data from the Affymetrix chip as described in the color key. The 100 most differentially expressed genes with a fold change of 1.5 and an adjusted $P < 0.05$ (EDI3 siRNA vs. control siRNA) were used to generate the heat map. The genes listed on the right are provided in **Table S1**, together with expression values. (**C**) Volcano plot showing the log2-fold change and p value of differentially expressed genes (EDI3 siRNA vs. control siRNA) in the Cancer Pathway Finder PCR array (SABiosciences). The black vertical line represents a fold change of one; whereas, the two pink lines represent a fold change of 1.5. The horizontal blue line represents the threshold of the p value which is set for $P = 0.05$. Three independent biological replicates were run as described in the methods section.

Table 1. Gene array results: Altered genes involved in attachment and migration

Gene	Probe Set	Fold Change	P value	Process
CAP1	213798_s_at	0.36	1.05E-05	Adhesion
ITGB1	1553678_a_at	0.37	2.63E-06	Adhesion; migration
ADAM10	202603_at	0.38	5.25E-07	Adhesion; migration
DCLK1	205399_at	0.40	1.17E-05	Migration
ITGB8	226189_at	0.43	8.32E-08	Adhesion
COL3A1	215076_s_at	0.44	1.78E-06	Adhesion
ITGB6	226535_at	0.46	5.13E-06	Adhesion
CADM1	209031_at	0.48	2.95E-07	Adhesion
CTGF	209101_at	0.50	5.01E-07	Adhesion; migration
VAV3	218807_at	0.53	7.94E-09	Adhesion; migration; angiogenesis
LAMB1	201505_at	0.53	9.55E-06	Adhesion; migration; differentiation
PRKCA	213093_at	0.55	1.95E-06	Migration
TWIST1	213943_at	0.61	5.25E-07	Migration
ITGA2	227314_at	0.64	2.75E-06	Adhesion
CXCR4	217028_at	0.64	4.57E-07	Migration
PLEKHA1	226247_at	2.87	9.77E-08	Proliferation; differentiation
TGFBR1	224793_s_at	3.12	8.91E-07	Differentiation; ruffle organization

analysis. Our experimental conditions led to an approximately 80% decrease in EDI3 RNA, protein, and activity (**Fig. 1A**) compared with the cells transfected with control siRNA. Clearly distinct expression patterns were obtained as a consequence of the EDI3 knockdown (**Fig. 1B** and **Table S1**). After false discovery rate correction, the gene array resulted in 269 significantly up- and 519 downregulated genes with at least a 1.5-fold difference from control (**Table S2**). A fraction of these genes (primarily those that were downregulated) are associated with cell migration and attachment (**Table 1**). Gene ontology (GO) analyses showed 34 overrepresented GO groups in the upregulated and 100 in the downregulated genes (**Table S3**). Among the downregulated genes, a remarkable fraction was associated with cell migration and attachment (**Table 2**). In contrast, none of the GO groups for the upregulated genes were associated with migration, spreading or cell attachment (**Table S3**).

In addition to the Affymetrix gene array, a second screen was performed using the Cancer Pathway Finder PCR array from SABiosciences. The expression of 84 cancer-related genes was compared in MCF-7 cells after knocking down EDI3. Of the nine genes that were significantly altered between the non-targeting control siRNA and EDI3 siRNA #1 samples, only seven had a fold change greater than 1.5 (**Fig. 1C** and **Table 3**). The two most significantly downregulated genes, SERPINB5 and TWIST1, are important for cell migration, thus supporting our previous findings of EDI3′s importance in this cellular process.[1] Three further genes that were downregulated in the EDI3 siRNA samples, namely ependymin related protein 1 (EPDR1), integrin α2 (CD49b) and integrin β1 (CD29), are all involved in cellular attachment, although the latter was not significantly altered. These changes and the importance of adhesion to the migration process prompted us to further investigate EDI3′s possible role in cellular adhesion.

Confirmation of EDI3′s influence on integrin β1 expression

Integrin β1 is a key subunit for cell attachment and integrin-mediated signaling. It can heterodimerize with any of 11 different α subunits, thus influencing matrix binding. To confirm the array results, qRT-PCR was used to measure *integrin β1* expression in five different cancer cell lines, including two breast cancer lines (MCF-7 and T47D), an ovarian carcinoma cell line (OVCAR-3) and two endometrial cancer cell lines (AN3-CA and MFE296) (**Fig. 2A**). In all cell lines, knocking down EDI3 resulted in a significant decrease in *integrin β1* expression. These data were confirmed using a second, independent siRNA oligo targeting EDI3′s exon 2 (siRNA #1 targets exon 13/14). EDI3 knockdown with oligo #2 was confirmed at RNA, protein and activity levels (**Fig.2 and Fig. S1**), and showed similar knockdown efficiency as oligo #1. Both siRNA species regulated *integrin β1* reproducibly down in all five analyzed cancer cell lines (**Fig. 2A**). Despite the similarity in EDI3 downregulation, in most cell lines

Table 2. Gene ontology (GO) analysis after EDI3 knockdown

GO Term: Number	Number of annotated genes	Number of significant genes	Number of expected genes	P value of enrichment
Integrin-mediated signaling pathway (GO:0007229)	190	13	3	0.000
Tight junction assembly (GO:0070830)	119	7	2	0.001
Axon guidance (GO:0007411)	1037	27	14	0.001
Cellular membrane organization (GO:0016044)	1074	33	14	0.002
Neuron projection development (GO:0035556)	1899	49	25	0.002
Cell-cell adhesion mediated by integrin (GO:0033631)	50	4	1	0.004
Neuron migration (GO:0001764)	254	9	3	0.007
Cell migration in sprouting angiogenesis (GO:0002042)	62	4	1	0.009

Table 3. Top genes found to be altered by PCR Array analysis

Gene	Fold up- or downregulation	P value	Function
SERPINB5	−2.20	<0.001	Migration
TWIST1	−1.96	0.047	Migration
ITGB1	−1.93	0.078	Adhesion
EPDR1	−1.87	0.015	Adhesion
FAS	−1.70	0.013	Apoptosis
ITGA2	−1.68	0.009	Adhesion
TIMP1	−1.28	0.009	Migration
BRCA1	−1.19	0.012	Cell cycle and DNA damage
RAF1	1.16	0.024	Signal transduction
PDGFA	1.69	0.035	Angiogenesis

siRNA EDI3 #1 had a greater effect on integrin expression than siRNA EDI3 #2. The reason for this discrepancy between the two siRNA oligos is unclear, but may be due to the two oligos targeting different splice variants of the EDI3 gene. However, for the current study, this discrepancy acts as an additional control to study EDI3′s role in adhesion. For further functional analyses, we focused on two well-characterized cell lines, MCF-7 and OVCAR-3. In agreement with the RNA data, protein levels of integrin β1 also decreased after knocking down EDI3 (**Fig. 2B**).

EDI3 influences cell adhesion

Since silencing of EDI3 was associated with decreased integrin β1, the key integrin subunit for cell attachment, we next investigated EDI3′s influence on α subunits known to heterodimerize with integrin β1. Except for the endometrial cell line, AN3-CA EDI3 siRNA #1 consistently decreased integrin α5 expression at both RNA and protein levels (**Fig. 2**). Integrin α5/β1 is the primary fibronectin receptor; therefore, EDI3′s influence on adhesion to fibronectin was investigated. Knockdown of EDI3 in MCF-7 cells decreased cell adhesion by approximately 50% compared with the control (**Fig. 3A**). In OVCAR-3 cells, loss of EDI3 after knockdown with oligo #1 significantly decreased cell attachment (**Fig. 3B**). Oligo # 2 had no effect on adhesion confirming the weak decrease in integrin α5/β1 expression observed after EDI3 knockdown in this particular cell line (**Fig. 2A**).

Role in cell spreading

After initial attachment and prior to migration, cells undergo a dynamic spreading process that is dependent on the cell's cytoskeletal structure. Due to EDI3′s role in both attachment and migration, we examined EDI3′s influence on cellular spreading. Actin was visualized using phalloidin in control cells or cells transfected with EDI3 siRNA 15, 30, 60, 120 and 240 min after plating on fibronectin. The results suggest a delay in spreading from 15 to 120 min, with the most striking differences after 60 min (**Fig. S2**). Therefore, further analyses and quantifications of the cell surface were performed 60 min after plating. In contrast to cell adhesion, both EDI3 siRNA species significantly decreased cell spreading in both MCF-7 (**Fig. 4A**) and OVCAR-3 cells (**Fig. 4B**), delaying the formation of cell protrusions. Confocal imaging at a higher magnification revealed the dramatic impact that loss of EDI3 has on the cytoskeletal organization (**Fig. 4C**).

Overexpression confirms EDI3′s influence on attachment and spreading

To confirm EDI3′s influence on adhesion and spreading, we used MCF-7 cells stably overexpressing EDI3, which were previously described.[1] EDI3 overexpression was associated with increased RNA and protein expression of both integrin β1 and integrin α5 (**Fig. 5A**), and enhanced attachment (**Fig. 5B**). To investigate EDI3′s role in cell spreading, overview images were taken 10 to 60 min after re-plating on fibronectin (**Fig. S3**) revealing the most obvious difference between EDI3 overexpressing and control cells after 30 min. Therefore, this time point was used for further analyses. As quantified in **Figure 5C**, higher EDI3 expression was associated with a significant increase in mean cell area. In addition, a greater distribution of cells with enlarged cell area was observed among the EDI3 overexpressing cells compared with those transfected with the empty vector. Finally, confocal microscopy of cells stained with phalloidin was used to visualize the accelerated spreading caused by EDI3 overexpression (**Fig. 5D**).

Discussion

Recently, we have shown that EDI3 (GPCPD1, GDE5), a key enzyme in choline metabolism, influences cell migration,[1] and is associated with worse prognosis in ovarian and endometrial cancers. Outside of this published work, very little is known about EDI3′s functions, and nothing on its potential role in cancer. Therefore, to obtain a comprehensive overview of the genes and possible processes influenced by EDI3, we performed gene array analysis after EDI3 knockdown in MCF-7 cells. Gene ontology analyses of the most significantly and differentially altered probe sets indicate an enrichment of genes involved in several biological processes. Interestingly, EDI3 knockdown was associated with an upregulation of genes involved in skeletal system development, which supports a previous study showing that EDI3 negatively regulates skeletal muscle development.[18] The downregulated genes were categorized into 100 GO groups, most notably intracellular signaling, metabolic processes, membrane organization, migration, integrin-mediated signaling, and skeletal system development. More specifically, knocking down EDI3 was associated with decreased expression of specific integrin subunits and other genes associated with cellular attachment, spreading and migration. Due to EDI3′s known role in migration, we were prompted to study a possible influence of its role in other integrin-mediated processes.

Integrins are membrane-bound receptors that facilitate attachment of cells, and link the ECM to the actin cytoskeleton. These receptors transmit signals from the external environment into the cell and vice versa – in so-called outside-in and inside-out signaling, respectively. The receptor itself is a heterodimer of one α and one β integrin subunit, the combination of which determines ECM preference. In the gene array analysis, the most significantly downregulated integrin subunit was *integrin β1*, a key subunit for integrin-mediated cell attachment to laminin, collagen and fibronectin. The decreased expression of *integrin β1* observed in the gene array was confirmed using a commercially

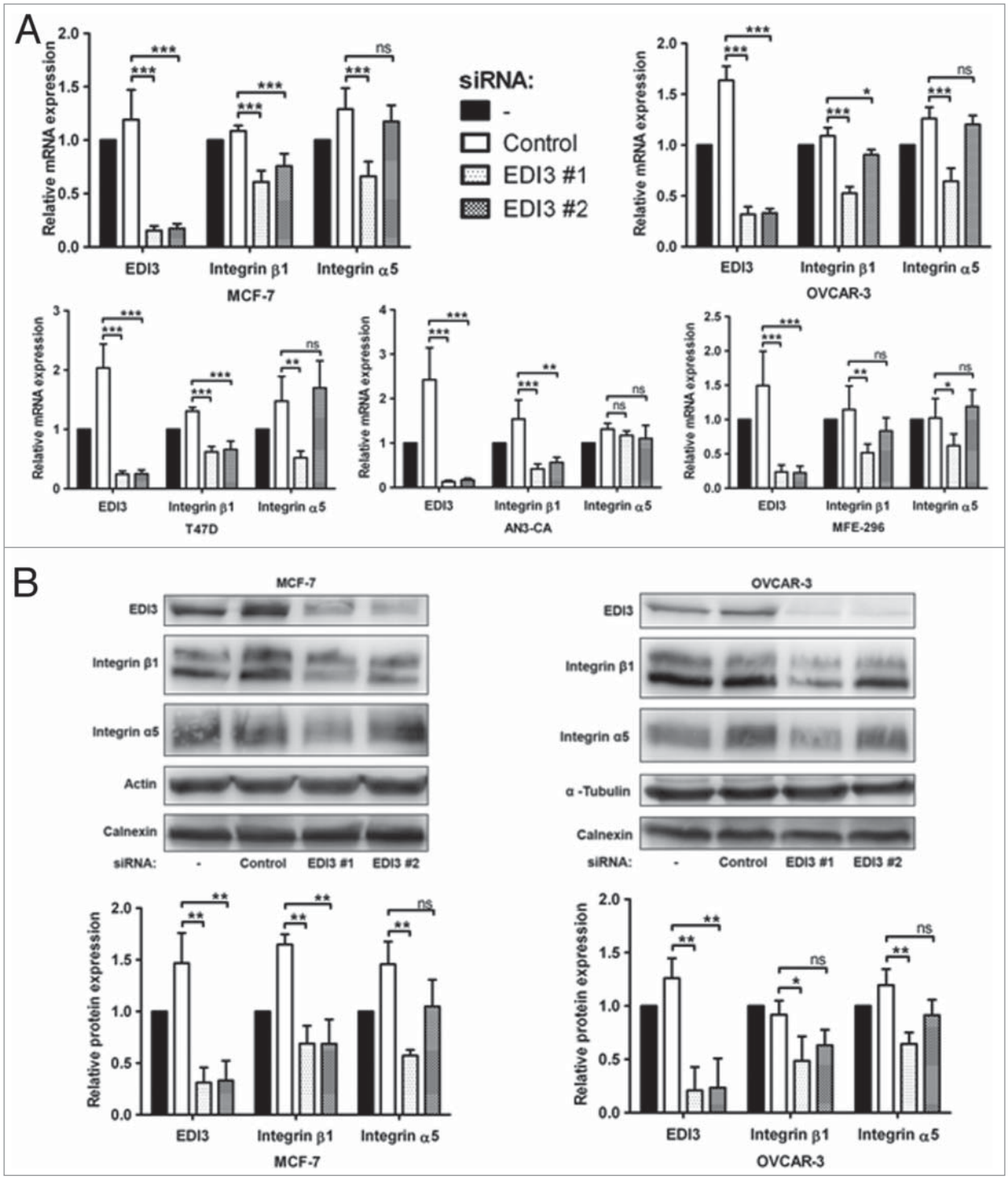

Figure 2. Downregulation of EDI3 reduces expression levels of integrin β1 and integrin α5. (**A**) Transfections of control siRNA and two EDI3-specific siRNAs were performed in five different cancer cell lines, namely OVCAR-3 (ovarian cancer), MCF-7 and T47D (both breast cancer), AN3-CA and MFE-296 (both endometrial cancer). RNA expression levels of *EDI3*, *integrin β1* and *integrin α5* were analyzed using quantitative real-time PCR. Values in graphs represent the mean ± SD from five independent experiments. (**B**) Cells were treated as described in (A) and protein expression levels of EDI3, integrin β1 and integrin α5 were analyzed by western blotting. Actin, α-tubulin and calnexin were used as loading controls. Shown are representative images and quantification values represent mean ± SD from three independent experiments.

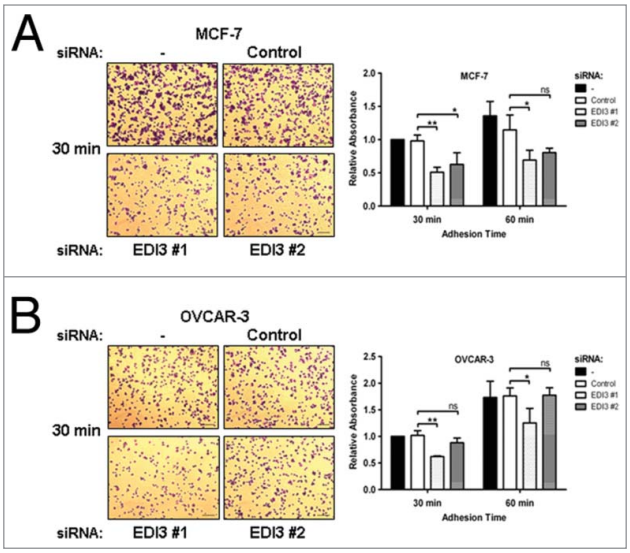

Figure 3. Downregulation of EDI3 impairs initial cell adhesion on fibronectin (FN). After siRNA knockdown for 72 h, (**A**) MCF-7 human breast cancer cells and (**B**) OVCAR-3 human ovarian cancer cells were harvested in suspension media containing 1% FBS and 0.5 mg/ml trypsin inhibitor, maintained in suspension for 1 h, and then re-plated on FN-coated 24-well plates for 30 or 60 min. Adherent cells were fixed and stained with crystal violet. Shown are representative phase contrast images taken with a 10x objective. Bars: 100 μm. After de-staining, the released crystal violet was quantified by absorbance measurements. Values in graphs represent mean ± SD from three independent experiments.

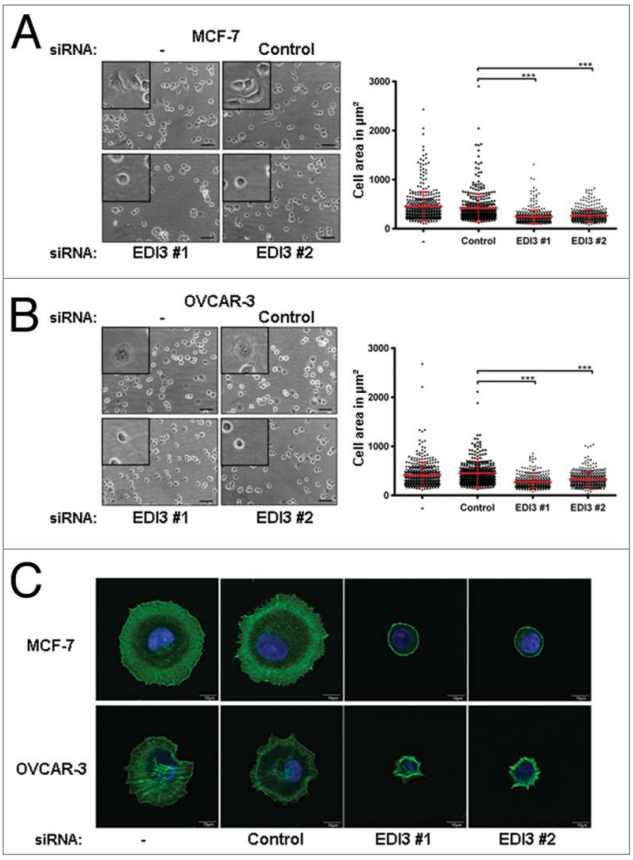

Figure 4. Downregulation of EDI3 impairs cell spreading. After siRNA knockdown of EDI3 for 72 h, (**A**) MCF-7 cells and (**B**) OVCAR-3 cells were harvested and maintained in suspension for 1 h, and then re-plated on FN-coated 24-well plates for 60 min. Adherent cells were fixed with 4% paraformaldehyde and phase contrast images of unstained cells were taken with a 20x objective. Bars: 50 μm. Magnified views are shown in the inserts. The cell area of 100 randomly chosen cells per condition and experiment from four independent experiments was quantified using ImageJ software and the mean cell size ± SD was calculated. Each point corresponds to the measured area of an individual cell. (**C**) SiRNA-treated MCF-7 and OVCAR-3 cells were harvested as described before and re-plated on FN-coated coverslips for 60 min. Adherent cells were fixed with 4% paraformaldehyde, and stained with phalloidin Alexa-488 (green) and DAPI (blue). Shown are representative single-cell images taken with a confocal laser scanning microscope using a 60x objective. Bars: 10 μm.

available PCR array and qRT-PCR in five different cancer cell lines. We found that knockdown of EDI3 showed decreased cell attachment and cell spreading on a fibronectin matrix. Finally, overexpression of EDI3 resulted in the opposite effects, namely enhanced attachment, spreading and integrin expression, thus confirming EDI3′s role in these processes.

For the analyses, two different siRNA species directed against different exons of EDI3 were used. Both oligos had similar effects on spreading in different cell lines. However, interpretation of the attachment results is more complex, and may be explained by differences in the consequences of EDI3 knockdown on integrin β1 expression, which varied between cell lines and the two siRNA species. An effect on cell adhesion was always observed when EDI3 siRNA significantly reduced integrin β1 expression. This was detected even when the reduction of integrin β1 was relatively small. For example, an 80% decrease in EDI3 expression with siRNA EDI3 #2 in MCF-7 cells resulted in a 30% reduction in *integrin β1* RNA and a concomitant decrease in integrin β1 protein (**Fig. 2**). In situations where no significant influence on integrin β1 was seen, such as for siRNA EDI3 #2 in OVCAR-3 cells, no influence on attachment was observed.

The difference in the effects of the two siRNA species (siRNA EDI3 #1 and #2) on attachment still remains difficult to interpret. Both oligos, which target different exons at the opposite ends of EDI3, led to a similar reduction in EDI3 RNA and protein expression in MCF-7 cells, but showed lower efficiency in OVCAR-3 (about 70%). One possible explanation is that this less efficient knockdown was close to a threshold required to influence cell adhesion. To clarify the situation, we additionally overexpressed EDI3 in MCF-7 cells, which consistently confirmed the association between EDI3 with increased integrin β1 and cell attachment. However, the mechanism by which EDI3 influences integrin β1 expression and the alterations seen in attachment and spreading remains unknown.

In our previous work, we showed that EDI3 directly influences PKCα expression.[1] Interestingly, activation of PKC in MCF-7 cells with phorbol esters was previously shown to increase surface expression of integrin β1 and attachment.[19] Another study, again in MCF-7 cells, showed a direct interaction between PKCα and integrin β1.[20] This interaction facilitated trafficking of integrin β1

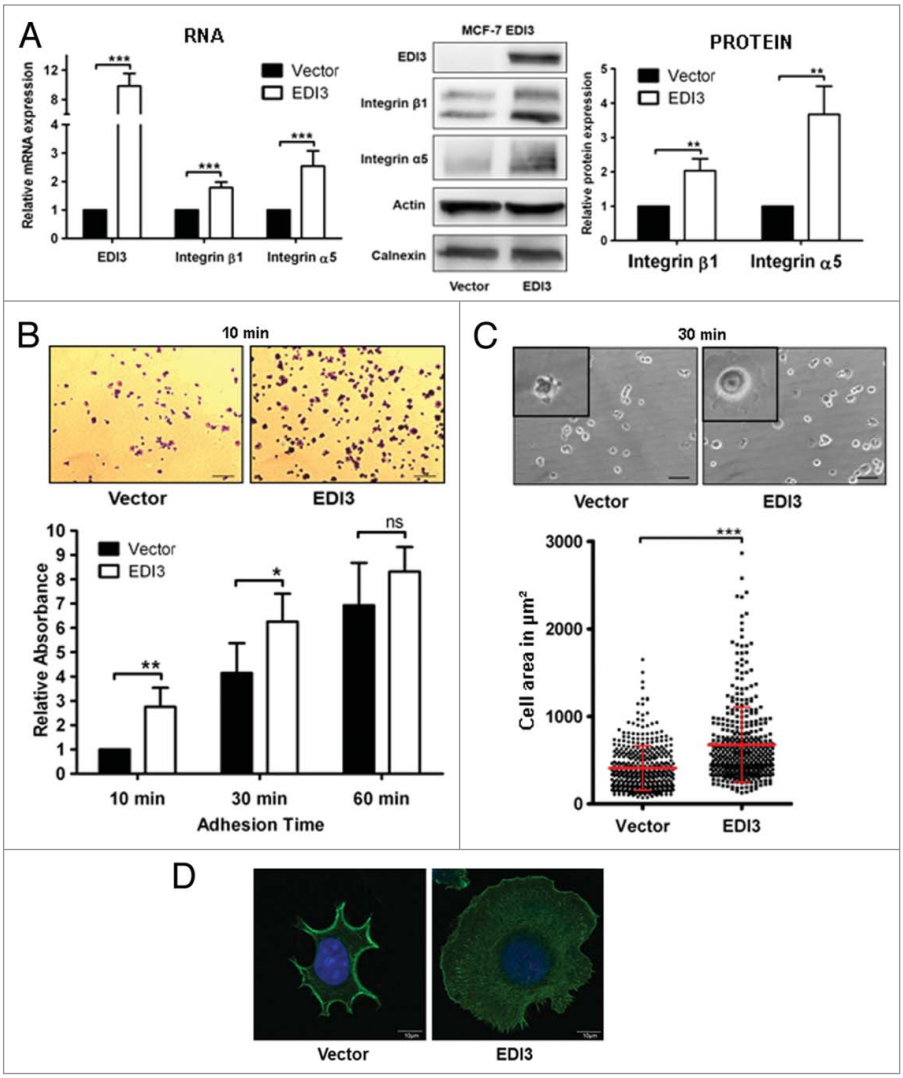

Figure 5. EDI3 overexpression leads to increased integrin α5β1 expression promoting both initial attachment and spreading. (**A**) In MCF-7 cells stably overexpressing EDI3, both RNA and protein expression levels of EDI3, integrin β1 and integrin α5 were analyzed using quantitative real-time PCR (n = 5) and western blotting (n = 3), respectively. For phenotypic analyses, the same cells were harvested and maintained in suspension for 1 h, and then re-plated on FN-coated culture dishes. (**B**) To analyze adhesion, cells were fixed and stained with crystal violet after 10, 30 and 60 min, and quantification was performed by absorbance measurements (n = 4). Bars: 100 μm. (**C**) To analyze spreading, cells were fixed with 4% paraformaldehyde after 30 min, and cell area was quantified based on phase contrast images (n = 4). The mean cell size ± SD was calculated from a total number of 400 randomly chosen cells gained from four independent experiments. Each point corresponds to the measured area of an individual cell. Bars: 50 μm. (**D**) To visualize the actin cytoskeleton, cells were fixed with 4% paraformaldehyde after 30 min, and stained with rhodamine phalloidin (green) and DAPI (blue) (n = 3). Bars: 10 μm. All images shown are representative and the values in graphs represent the mean ± SD of at least three independent experiments.

to the plasma membrane and was associated with increased cell motility. Furthermore, chemically inhibiting PKC with calphostin C decreased the protein and RNA expression of integrin α5β1.[21] The decreased expression of both proteins, which are critical for migration, attachment and spreading, may be a plausible explanation for EDI3′s effect on these cellular processes and needs to be further investigated. EDI3′s influence on PKCα and the association between PKCα and integrin β1 were both observed in the non-metastatic MCF-7 breast cancer cell line. We previously showed that EDI3 also influences migration and choline metabolism in the more metastatic cell lines, MDA-MB-231 (breast cancer) and AN3-CA (endometrial cancer).[1] In addition, unpublished data indicate that *EDI3* RNA expression is higher in the MDA-MB-231 cells compared with MCF-7. How this higher EDI3 expression influences PKCα, integrin expression, adhesion, and spreading will be explored in future studies.

To date, seven glycerophosphodiesterases (GDEs) have been described; however, with the exception of EDI3 and GDE2 which also cleaves GPC, none have been implicated in cancer or cancer-related processes. GDE2 expression was shown to be associated with more metastatic ER negative breast cancer.[22] The authors went on to correlate elevated GDE2 with the levels of choline metabolites, together with choline kinase α and phospholipase D expression. However, no mechanism was provided as to how high GDE2 levels contribute to worse prognosis. Like GDE2, EDI3′s enzymatic activity produces choline and glycerol-3-phosphate; unlike GDE2 and all other GDEs, EDI3 is cytoplasmic rather than membrane-bound, suggesting that their functions are not redundant. Choline, an essential nutrient obtained from diet or from de novo synthesis, can be oxidized to the critical methyl donor, betaine; or further metabolized via the Kennedy pathway to phosphatidylcholine (PtdCho), which constitutes approximately 50% of all membranes, and is therefore critical for their structural integrity.[23,24] Hydrolysis of PtdCho by different phospholipases produces potent signaling lipids, such as lysophosphatidylcholine, phosphatidic acid (PA) and diacylglycerol (DAG). Both PA and DAG are also direct downstream metabolites of EDI3′s second product, glycerol-3-phosphate.

Although not dramatic, knockdown of EDI3 was associated with a decrease in specific PtdCho and PA species.[1] PA, formed from the hydrolysis of PtdCho by phospholipase D (PLD), was previously shown to be important in both cell spreading and migration.[25-27] Chae et al. showed that PA anchors the small GTPase Rac1 to the plasma membrane in OVCAR-3 cells. The interaction between Rac1 and PA was shown to facilitate the activation of Rac1

downstream targets, such as p21 activated kinase, and regulate integrin-dependent cell spreading and migration.[25] Interestingly, PLD2 activity and PA were also shown to negatively regulate early spreading, via PA's ability to regulate the activity of myosin phosphatase, an enzyme controlling myosin contractility.[26,27] Inhibiting PLD and thus PA production in CHO cells led to myosin dephosphorylation, which relaxed the contractile force at the cell's periphery accelerating cell spreading. These, and similar studies suggest that the role of PA in spreading and migration is complex and also not fully elucidated, and whether EDI3′s role in spreading is via PA needs to be investigated.

In conclusion, we have shown that EDI3 influences cell spreading and attachment, thereby linking choline metabolism to integrin expression, organization of the actin cytoskeleton and cancer cell phenotypes.

Materials and Methods

Cell culture

MCF-7 human breast cancer cells were purchased from the German Collection of Microorganisms and Cell Cultures and maintained in Dulbecco's modified medium (DMEM; PAN-Biotech) supplemented with 10% heat-inactivated fetal bovine serum (PAN-Biotech), 1% sodium pyruvate (Sigma), 0.5% non-essential amino acids (Gibco), and 0.1% insulin (Sigma). MCF-7 cells stably transfected with pCMV6-GFP or pCMV6-GFP-EDI3[1] were purchased from AMS Bio and maintained in DMEM supplemented with 10% fetal bovine serum, 0.1% insulin and 0.5 mg/ml G418 (Sigma). OVCAR-3 human ovarian cancer cells obtained from ATCC were maintained in RPMI media supplemented with 20% fetal bovine serum and 0.1% insulin. All cells were grown in a humidified incubator at 37°C with 5% CO_2.

RNA interference

To silence EDI3, cells were transfected with two Stealth RNAi siRNA oligos specific for human EDI3 (Invitrogen) as previously described.[1] Briefly, 0.5×10^6 cells in 2.5 ml antibiotic-free medium were added to each well of a six-well plate containing 500 μl Opti-MEM, 20 nM siRNA oligos and 5 μl Lipofectamine RNAiMAX (Invitrogen). Stealth RNAi siRNA negative control low/med GC (Invitrogen) was used to control for off-target effects of the RNAi process. Cells were incubated for 72 h to ensure knockdown at the RNA and protein level and then used for the described experiments.

Gene array

MCF-7 cells were transfected with either non-targeting control siRNA or EDI3 siRNA #1 for gene array analysis. Three independent biological replicates, each with three technical replicates were prepared and samples stored in RNA later until analysis. RNA was isolated using Qiagen's RNeasy kit according to the manufacturer's instructions and quantified using a NanoDrop N-1000 spectrophotometer (NanoDrop, Wilmington, DE, USA). Its integrity was confirmed with a standard sense automated gel electrophoresis system (Experion, Bio-Rad). RNA was only used for analysis if the RNA quality indicator (RQI) number was higher than 8. Further analysis was performed as previously described.[28] Briefly, first-strand cDNA was synthesized using 100 ng total RNA using an oligo-dT primer with an attached T7 promoter sequence, followed by the complementary second strand. The double-stranded cDNA molecule was used for in vitro transcription using Genechip 30 IVT Express Kit. A biotinylated nucleotide analog, which serves as a label for the message, was incorporated during synthesis of amplified RNA (aRNA). The aRNA was then purified using magnetic beads and 15 μg of aRNA was fragmented with fragmentation buffer. Subsequently, 12.5 μg fragmented aRNA was hybridized with Affymetrix Human Genome U133 plus 2.0 arrays following the manufacturer's instructions. The chips were placed in a GeneChip Hybridization Oven-645 for 16 h at 60 rpm and 45°C. AffymetrixHWS kits were used on a Genechip Fluidics Station-450 to stain and wash the chips. For scanning, the Affymetrix GeneChip Scanner-3000–7G was used. All reagents and instruments were acquired from Affymetrix (Affymetrix). The generated CEL files were used for further statistical analysis and all data were deposited in ArrayExpress upon acceptance of the manuscript.

PCR array

The Cancer Pathway Finder PCR array from SABiosciences was run according to the manufacturer's directions. Briefly, RNA was isolated from MCF-7 cells transfected with either control siRNA or EDI3 siRNA #1. cDNA was made using the RT^2 First Strand Kit (SABiosciences) with 1 μg of total RNA. The cDNA was added to SYBR Green RT^2 qPCR master mix (SABiosciences) and each sample was loaded onto a single 96-well plate containing primer sequences for 84 genes involved in cancer progression, housekeeping genes and pre-designed positive and negative controls. The PCR reaction was run on an ABI 7500 Fast Real-Time PCR System (Applied Biosystems) according to the instructions provided by SABiosciences for the SYBR Green qPCR Mastermix. Three independent biological replicates were performed and data analyzed using the analysis template provided by SABiosciences.

Quantitative real-time PCR

Total RNA from cells was isolated using Qiazol (Qiagen) following the manufacturer's instructions. Two μg total RNA was transcribed into cDNA using high-capacity cDNA Reverse Transcription Kit (Applied Biosystems). Quantitative real-time PCR analysis was performed using Quantitect SYBR Green RT-PCR kit (Qiagen), custom-designed Quantitect primer assays [β-Actin: QT1680476; EDI3: QT00066598; Integrin β1: QT00068124; Integrin α5: QT00080871 (Qiagen)], and the ABI 7500 Fast Real-Time PCR System (Applied Biosystems) according to the manufacturer's protocol. Relative quantification was calculated using the $2^{-\Delta\Delta Ct}$ method with β-actin as the endogenous control.

Western blot analysis

Whole cell lysates were collected in RIPA lysis buffer (1% (v/v) NP-40, 150 mM NaCl, 20 mM Tris/HCl (pH 7.4), 1 mM EDTA, 10 mM NaF, 1 mM $ZnCl_2$, 1 mM $MgCl_2$, 1 mM Na_3VO_4, 10% (v/v) Glycerol) with protease and phosphatase

inhibitors (Sigma) and protein content was quantified using the BCA Protein Assay kit (Thermo Scientific). Protein samples were separated on 8% SDS polyacrylamide gels using the mini-PROTEAN Tetra Electrophoresis System (Bio-Rad) and transferred to PVDF membranes (Perkin-Elmer). Primary antibody incubation was performed overnight at 4°C with the following antibodies used at a dilution of 1:1,000 – custom-made mouse monoclonal anti-EDI3 (AMS Bio), anti-β-Actin (Sigma), anti-α-Tubulin, anti-Calnexin, anti-Integrin α5, anti-Integrin β1 (all from Cell Signaling). HRP-conjugated secondary antibodies (anti-rabbit IgG and anti-mouse IgG) were purchased from Cell Signaling and used at a dilution of 1:1,000 for 2 h at room temperature. All images were taken on a Vilber Fusion Fx7 imager (Vilber Lourmat) using chemiluminescence (Perkin-Elmer) for detection and bands were quantified using ImageJ software (National Institute of Health).

EDI3 activity assay

EDI3′s enzymatic activity was determined in vitro using an enzyme-coupled spectrophotometric assay as previously described.[1] Briefly, cell lysates diluted in assay buffer (50 mM TRIS-HCl, 0.14 M NaCl and 2 mM $MgCl_2$) were incubated with the substrate glycerophosphocholine and a reaction mix containing 100 μM Amplex Red Reagent, 2 U/ml horseradish peroxidase and 0.2 U/ml choline oxidase (Invitrogen). Upon incubation at 37°C, choline was formed by cleavage of the added substrate. The produced choline was oxidized to betaine and H_2O_2, finally leading to the conversion of Amplex Red to the fluorescent product, resorufin, which could be measured at 595 nm using a microplate reader (TECAN SpectraFluor Plus).

Cell suspension and re-plating assays

For experiments using a fibronectin matrix, plastic dishes, multi-well cell culture plates or glass coverslips were coated with 20 μg/ml human fibronectin (BD Biosciences) at 4°C overnight. Before use, the coated cell culture ware was blocked with 1% bovine serum albumin (Carl Roth) for 1 h at room temperature and rinsed with 1 × PBS.

For re-plating assays, cells were detached using 0.5% Trypsin/EDTA (PAN-Biotech) and diluted in suspension media (normal media containing only 1% fetal bovine serum) to which 0.5 mg/ml soybean trypsin inhibitor type II (Sigma) was added. Cells were collected by centrifugation at 500 × g for 5 min, resuspended in fresh suspension media and then kept in suspension for 1 h at 37°C using a MacsMix Rotator (Miltenyi Biotec). After rotation, the cells were re-plated on fibronectin. Both the maintenance in 1% serum and the recovery period at 37°C were essential for adequate adhesion and spreading.

Cell adhesion assay

For adhesion assays, suspension cells were re-plated on fibronectin-coated 96-well plates (5×10^4 cells per well). To visualize cell adhesion after 15 to 60 min, cells were rinsed with 1x PBS and then fixed and stained in a 0.1% (w/v) crystal violet (Sigma) solution containing 10% (v/v) ethanol for 20 min at room temperature. After staining, pictures were taken using a phase contrast microscope (NIKON eclipse T5100) and a 10x objective. Cells were de-stained using 0.2% Triton X-100 (Sigma) and the released crystal violet was quantified by measuring the absorbance at 570 nm using a microplate reader (TECAN SpectraFluor Plus).

Cell spreading assay

For spreading assays, suspension cells were re-plated on fibronectin-coated 24-well plates (1.5×10^5 cells per well) in triplicate. After 30 to 60 min, cells were rinsed with 1 × PBS and adherent cells were fixed with 4% paraformaldehyde (Carl Roth) for 20 min at room temperature. To quantify cell spreading, three images of the fixed and unstained cells were taken per well using a phase contrast microscope (NIKON eclipse T5100) and a 20x objective. Cell surface area of 100 randomly chosen cells per condition and experiment was measured manually using ImageJ software. The mean cell size was calculated from four independent experiments; i.e., in total 400 measured cells per condition. Mann Whitney U (two sided) test was applied to analyze the statistical significance of the data.

Immunocytochemistry

To visualize the cytoskeleton during cell spreading, suspension cells were re-plated on 14mm-diameter fibronectin-coated coverslips (Menzel) in a 24-well format. After the indicated attachment times, cells were rinsed with 1 × PBS and fixed with 4% paraformaldehyde for 20 min at room temperature. After washing three times with PBS, cells were permeabilized with 0.5% Triton X-100 for 10 min. To visualize cell nuclei, cells were stained with DAPI (1:10,000; Invitrogen) for 15 min. For visualization of actin filaments, cells were stained with either phalloidin Alexa-488 or rhodamine-labeled phalloidin for 45 min at room temperature (1:250; Invitrogen). Slides were examined under a confocal laser scanning microscope (Olympus CLSM FV1000). Overview and single-cell pictures were taken with a 20x and a 60x objective, respectively.

Statistical analysis

Unless otherwise stated, student's paired *t* test (two-tailed) was used to compare the difference between two groups where $P < 0.05$ was considered significant ($^*P < 0.05$; $^{**}P < 0.01$; $^{***}P < 0.001$). The gene array analyses were performed using the statistical programming language 'R-version 3.0.2'. For the normalization of 18 Affymetrix gene expression arrays, the Robust Multi-array Average (RMA) algorithm[29] was used that applies background correction, log2 transformation, quantile normalization and a linear model fit to the normalized data to obtain a value for each probe set on each array. Differential expression was calculated using the R package limma.[30] Here, the combined information of the complete set of genes is used by an empirical Bayes adjustment of the variance estimates of single genes. This form of a moderated *t* test is abbreviated here as 'Limma *t* test'. The resulting p-values were multiplicity-adjusted to control the false discovery rate (FDR) by the Benjamini–Yekutieli procedure. For generating lists of significant genes the p-value cut-off 0.01 and fold-change cut-off 1.5 was used. Significance of enrichment of GO groups with differentially expressed genes was calculated with Fisher's exact test and the elim algorithm.[31] For generating lists of significant GO groups the p-value cut-off 0.01 was used.

Disclosure of Potential Conflicts of Interest

The authors have declared that no conflicts of interest exist.

The funders had no role in study design, data collection and analysis, decision to publish, or preparation of the manuscript.

Acknowledgments

We thank Agapios Sachinidis at the Center of Physiology and Pathophysiology of the Medical Faculty at the University of Cologne for performing the gene microarray analysis. This project was supported by the BMBF (German Federal Ministry of Education and Research) project Virtual Liver (FK2 0315739).

Supplemental Materials

Supplemental data for this article can be access on the publisher's website.

References

1. Stewart JD, Marchan R, Lesjak MS, Lambert J, Hergenroeder R, Ellis JK, Lau CH, Keun HC, Schmitz G, Schiller J, et al. Choline-releasing glycerophosphodiesterase EDI3 drives tumor cell migration and metastasis. Proc Natl Acad Sci U S A 2012; 109:8155-60; PMID:22570503; http://dx.doi.org/10.1073/pnas.1117654109
2. Marchan R, Lesjak MS, Stewart JD, Winter R, Seeliger J, Hengstler JG. Choline-releasing glycerophosphodiesterase EDI3 links the tumor metabolome to signaling network activities. Cell Cycle 2012; 11:4499-506; PMID:23114620; http://dx.doi.org/10.4161/cc.22544
3. Tayebati SK, Amenta F. Choline-containing phospholipids: relevance to brain functional pathways. Clin Chem Lab Med 2013; 51:513-21; PMID:23314552; http://dx.doi.org/10.1515/cclm-2012-0559
4. Corbin KD, Zeisel SH. Choline metabolism provides novel insights into nonalcoholic fatty liver disease and its progression. Curr Opin Gastroenterol 2012; 28:159-65; PMID:22134222; http://dx.doi.org/10.1097/MOG.0b013e32834e7b4b
5. Lombardi B, Pani P, Schlunk FF. Choline-deficiency fatty liver: impaired release of hepatic triglycerides. J Lipid Res 1968; 9:437-46; PMID:5725875
6. Aboagye EO, Bhujwalla ZM. Malignant transformation alters membrane choline phospholipid metabolism of human mammary epithelial cells. Cancer Res 1999; 59:80-4; PMID:9892190
7. Ackerstaff E, Glunde K, Bhujwalla ZM. Choline phospholipid metabolism: a target in cancer cells? J Cell Biochem 2003; 90:525-33; PMID:14523987; http://dx.doi.org/10.1002/jcb.10659
8. Glunde K, Ackerstaff E, Mori N, Jacobs MA, Bhujwalla ZM. Choline phospholipid metabolism in cancer: consequences for molecular pharmaceutical interventions. Mol Pharm 2006; 3:496-506; PMID:17009848; http://dx.doi.org/10.1021/mp060067e
9. Glunde K, Bhujwalla ZM, Ronen SM. Choline metabolism in malignant transformation. Nat Rev Cancer 2011; 11:835-48; PMID:22089420
10. Iorio E, Mezzanzanica D, Alberti P, Spadaro F, Ramoni C, D'Ascenzo S, Millimaggi D, Pavan A, Dolo V, Canevari S, et al. Alterations of choline phospholipid metabolism in ovarian tumor progression. Cancer Res 2005; 65:9369-76; PMID:16230400; http://dx.doi.org/10.1158/0008-5472.CAN-05-1146
11. Ackerstaff E, Pflug BR, Nelson JB, Bhujwalla ZM. Detection of increased choline compounds with proton nuclear magnetic resonance spectroscopy subsequent to malignant transformation of human prostatic epithelial cells. Cancer Res 2001; 61:3599-603; PMID:11325827
12. Eliyahu G, Kreizman T, Degani H. Phosphocholine as a biomarker of breast cancer: molecular and biochemical studies. Int J Cancer 2007; 120:1721-30; PMID:17236204; http://dx.doi.org/10.1002/ijc.22293
13. Hattingen E, Bähr O, Rieger J, Blasel S, Steinbach J, Pilatus U. Phospholipid metabolites in recurrent glioblastoma: in vivo markers detect different tumor phenotypes before and under antiangiogenic therapy. PLoS One 2013; 8:e56439; PMID:23520454; http://dx.doi.org/10.1371/journal.pone.0056439
14. Gallego-Ortega D, Gómez del Pulgar T, Valdés-Mora F, Cebrián A, Lacal JC. Involvement of human choline kinase alpha and beta in carcinogenesis: a different role in lipid metabolism and biological functions. Adv Enzyme Regul 2011; 51:183-94; PMID:21035492; http://dx.doi.org/10.1016/j.advenzreg.2010.09.010
15. Iorio E, Ricci A, Bagnoli M, Pisanu ME, Castellano G, Di Vito M, Venturini E, Glunde K, Bhujwalla ZM, Mezzanzanica D, et al. Activation of phosphatidylcholine cycle enzymes in human epithelial ovarian cancer cells. Cancer Res 2010; 70:2126-35; PMID:20179205; http://dx.doi.org/10.1158/0008-5472.CAN-09-3833
16. Ramírez de Molina A, Gutiérrez R, Ramos MA, Silva JM, Silva J, Bonilla F, Sánchez JJ, Lacal JC. Increased choline kinase activity in human breast carcinomas: clinical evidence for a potential novel antitumor strategy. Oncogene 2002; 21:4317-22; PMID:12082619; http://dx.doi.org/10.1038/sj.onc.1205556
17. Ramírez de Molina A, Rodríguez-González A, Gutiérrez R, Martínez-Piñeiro L, Sánchez J, Bonilla F, Rosell R, Lacal J. Overexpression of choline kinase is a frequent feature in human tumor-derived cell lines and in lung, prostate, and colorectal human cancers. Biochem Biophys Res Commun 2002; 296:580-3; PMID:12176020; http://dx.doi.org/10.1016/S0006-291X(02)00920-8
18. Okazaki Y, Ohshima N, Yoshizawa I, Kamei Y, Mariggiò S, Okamoto K, Maeda M, Nogusa Y, Fujioka Y, Izumi T, et al. A novel glycerophosphodiester phosphodiesterase, GDE5, controls skeletal muscle development via a non-enzymatic mechanism. J Biol Chem 2010; 285:27652-63; PMID:20576599; http://dx.doi.org/10.1074/jbc.M110.106708
19. Rosfjord EC, Maemura M, Johnson MD, Torri JA, Akiyama SK, Woods VL Jr, Dickson RB. Activation of protein kinase C by phorbol esters modulates alpha2-beta1 integrin on MCF-7 breast cancer cells. Exp Cell Res 1999; 248:260-71; PMID:10094832; http://dx.doi.org/10.1006/excr.1998.4390
20. Ng T, Shima D, Squire A, Bastiaens PI, Gschmeissner S, Humphries MJ, Parker PJ. PKCalpha regulates beta1 integrin-dependent cell motility through association and control of integrin traffic. EMBO J 1999; 18:3909-23; PMID:10406796; http://dx.doi.org/10.1093/emboj/18.14.3909
21. Guo HB, Lee I, Bryan BT, Pierce M. Deletion of mouse embryo fibroblast N-acetylglucosaminyltransferase V stimulates alpha5beta1 integrin expression mediated by the protein kinase C signaling pathway. J Biol Chem 2005; 280:8332-42; PMID:15615721; http://dx.doi.org/10.1074/jbc.M413532200
22. Cao MD, Döpkens M, Krishnamachary B, Vesuna F, Gadiya MM, Lønning PE, Bhujwalla ZM, Gribbestad IS, Glunde K. Glycerophosphodiester phosphodiesterase domain containing 5 (GDPD5) expression correlates with malignant choline phospholipid metabolite profiles in human breast cancer. NMR Biomed 2012; 25:1033-42; PMID:22279038; http://dx.doi.org/10.1002/nbm.2766
23. Li Z, Vance DE. Phosphatidylcholine and choline homeostasis. J Lipid Res 2008; 49:1187-94; PMID:18204095; http://dx.doi.org/10.1194/jlr.R700019-JLR200
24. Zeisel SH. Choline: critical role during fetal development and dietary requirements in adults. Annu Rev Nutr 2006; 26:229-50; PMID:16848706; http://dx.doi.org/10.1146/annurev.nutr.26.061505.111156
25. Chae YC, Kim JH, Kim KL, Kim HW, Lee HY, Heo WD, Meyer T, Suh PG, Ryu SH. Phospholipase D activity regulates integrin-mediated cell spreading and migration by inducing GTP-Rac translocation to the plasma membrane. Mol Biol Cell 2008; 19:3111-23; PMID:18480413; http://dx.doi.org/10.1091/mbc.E07-04-0337
26. Du G, Frohman MA. A lipid-signaled myosin phosphatase surge disperses cortical contractile force early in cell spreading. Mol Biol Cell 2009; 20:200-8; PMID:18946083; http://dx.doi.org/10.1091/mbc.E08-06-0555
27. Su W, Yeku O, Olepu S, Genna A, Park JS, Ren H, Du G, Gelb MH, Morris AJ, Frohman MA. 5-Fluoro-2-indolyl des-chlorohalopemide (FIPI), a phospholipase D pharmacological inhibitor that alters cell spreading and inhibits chemotaxis. Mol Pharmacol 2009; 75:437-46; PMID:19064628; http://dx.doi.org/10.1124/mol.108.053298
28. Krug AK, Kolde R, Gaspar JA, Rempel E, Balmer NV, Meganathan K, Vojnits K, Baquié M, Waldmann T, Ensenat-Waser R, et al. Human embryonic stem cell-derived test systems for developmental neurotoxicity: a transcriptomics approach. Arch Toxicol 2013; 87:123-43; PMID:23179753; http://dx.doi.org/10.1007/s00204-012-0967-3
29. Irizarry RA, Hobbs B, Collin F, Beazer-Barclay YD, Antonellis KJ, Scherf U, Speed TP. Exploration, normalization, and summaries of high density oligonucleotide array probe level data. Biostatistics 2003; 4:249-64; PMID:12925520; http://dx.doi.org/10.1093/biostatistics/4.2.249
30. Smyth GK, Michaud J, Scott HS. Use of within-array replicate spots for assessing differential expression in microarray experiments. Bioinformatics 2005; 21:2067-75; PMID:15657102; http://dx.doi.org/10.1093/bioinformatics/bti270
31. Alexa A, Rahnenführer J, Lengauer T. Improved scoring of functional groups from gene expression data by decorrelating GO graph structure. Bioinformatics 2006; 22:1600-7; PMID:16606683; http://dx.doi.org/10.1093/bioinformatics/btl140